J Seismol (2019) 23:493–504
https://doi.org/10.1007/s10950-019-09819-0

ORIGINAL ARTICLE

SN-CAST: seismic network capability assessment software tool for regional networks-examples from Ireland

Martin Möllhoff · Christopher J. Bean · Brian J. Baptie

Received: 4 April 2018 / Accepted: 31 January 2019 / Published online: 14 February 2019

Abstract Event detection capability plays an important role in the operation of seismic observatories and temporary networks. The magnitude threshold for the detection of seismic events with a given network geometry is frequently derived from the observed magnitude of completeness. However, the latter might be unknown for regions that have not been monitored previously or where the observed seismicity rate is low. We present the open-source Python program SN-CAST with which the geographical distribution of event detection capability can be calculated as a function of station coordinates and station ambient noise amplitudes. The method employs the local magnitude scale, and hence is mainly applicable to regional networks with an aperture of less than about 1000 km. The attenuation characteristics of the study region need to be derived independently or be known *a priori*. SN-CAST can easily be employed to determine network performance in quasi real-time if station data streams are available. It can also be used for designing the geometry of new networks or assessing the effect of adding or removing stations from an existing network. We present examples from the Irish National Seismic Network (https://www.insn.ie), which operates in a region of low seismicity and large variations in ocean and wind-generated seismic noise. The seismicity in Ireland is too low to allow the calculation of a magnitude of completeness for comparison with the derived capability maps. However, the maps are in good agreement with the location and magnitude of detected local and regional earthquakes demonstrating that SN-CAST is a reliable tool for assessing the detection capability of seismic networks.

Keywords Seismic network · Event · Detection · Magnitude · Performance · Noise

M. Möllhoff · C. J. Bean
Geophysics Section, Dublin Institute for Advanced Studies, School of Cosmic Physics, 5 Merrion Square, Dublin 2, Ireland
e-mail: martin@dias.ie

B. J. Baptie
British Geological Survey, The Lyell Centre, Research Avenue South, Edinburgh, EH14 4AP, Scotland

1 Introduction

The magnitude detection threshold of a seismic network is of great importance for the general operation of seismic observatories, the monitoring of induced seismicity, the geometric design of new networks, and assessing the effect of station failures or network upgrades. Different methods exist to calculate the detection capability of networks. A simple approach is to calculate the magnitude of completeness M_c which is the minimum magnitude above which all earthquakes within a certain region are reliably recorded. M_c can be determined from an event catalog by finding the point of deviation from the power law scaling of the Gutenberg-Richter frequency-magnitude distribution, see, for example, (Nanjo et al. 2010; Fischer and Bachura 2014; Schultz et al. 2015) and (Mahani et al. 2016). Another approach for determining network capability is to derive it using theoretical modeling, for example, with numerical simulations of ground motions (D'Alessandro et al. 2013; Mahani et al. 2016), rupture, and wave propagation modeling (Stabile et al. 2013) or earthquake spectra simulations (D'Alessandro et al. 2013; Schultz et al. 2015). These theoretical methods are frequently combined with a statistical analysis of station noise measurements because they have a major influence on network capability (e.g., D'Alessandro et al. (2013), Stabile et al. (2013), Fischer and Bachura (2014), Schultz et al. (2015), Demuth et al. (2016), and Mahani et al. (2016)).

Here, we develop a different approach that is based purely on measured noise statistics and an assumed local magnitude (M_L) scale for the area of interest. The goal of SN-CAST is to provide a tool that can be employed readily without the need for numerical modeling and can be applied to previously unmonitored areas or areas of low seismicity. SN-CAST calculates the geographical distribution of network capability which can easily be plotted to provide network capability maps. In the next section, we describe the method and give examples of its implementation, employing SN-CAST to provide capability maps for the Irish National Seismic Network (INSN (1993), https://www.insn.ie).

2 Method and implementation

The detection and location capability of a seismic network depends on many factors including network geometry, the detection threshold at the individual stations, and the minimum number N of station records required to reliably exclude false detections and declare an event to have occurred. The detection threshold at individual stations is usually considered to be surpassed once the signal-to-noise ratio (SNR) between maximum event amplitude A and background noise amplitude d is larger than 3 (Baillard et al. 2014; Gaci 2014; Stork et al. 2014). However, in order to ensure unambiguous event detection in some studies, a SNR threshold as high as 10 is chosen (e.g., Schultz et al. (2015) and Mahani et al. (2016)).

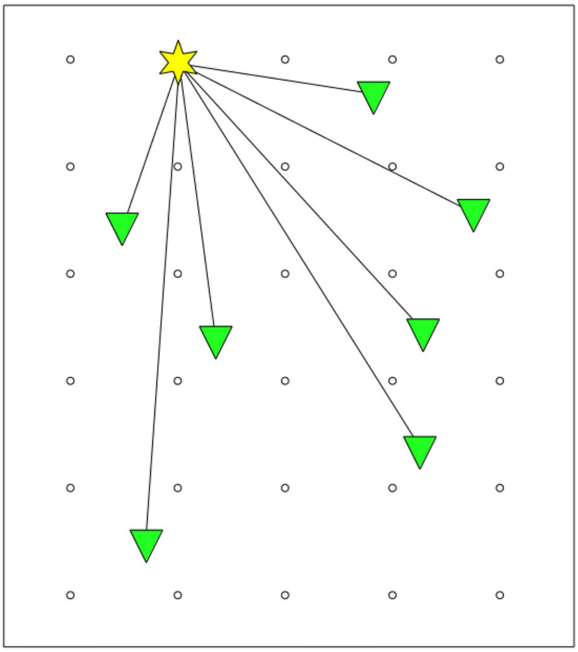

Fig. 1 Sketch of the grid method to calculate network capability. Small circles represent hypothetical epicenters, green triangles show station locations, and the star represents a grid point for which minimum detectable M_L is calculated

SN-CAST only requires station coordinates and station noise amplitudes d as input. The latter should be representative of frequencies that dominate local and regional event records of interest, typically 2–10 Hz (Demuth et al. 2016). A grid of hypothetical epicenters covering the network region (see small circles in Fig. 1), is used to calculate, for each grid point, the minimum detectable M_L as follows:

1. Calculate the hypocentral distances R between the grid point and each station. For network capability estimation at regional scale epicentral distances can be used as an approximation for hypocentral distances.
2. For a range of values, calculate for each station the maximum ground displacement amplitude A from the equation for the M_L scale, see below for details.
3. Find the smallest M_L value for which the condition $A > 3d$ is met for at least N stations.

The amplitude values A in step 2 can be calculated for a seismic event registered at a station with hypocentral distance R using the equation for the M_L scale (Havskov and Ottemöller 2010) as follows:

$$M_L = \log(A) + a \cdot \log(R) + b \cdot R + c \quad (1)$$

where A is the maximum ground displacement amplitude measured with a Wood-Anderson (W-A) seismometer and the parameters a, b, and c are constants representing respectively geometrical spreading, attenuation and the base level which is used to anchor the scale to the original definition by Richter (1935). The three latter parameters depend on local conditions, resulting in different M_L scales for different geographical regions. The first M_L scale was formulated by Richter (1935) for Southern California and the subsequently improved version by Hutton and Boore (1987) is as follows:

$$M_L = \log(A) + 1.11 \cdot \log(R) + 0.00189 \cdot R - 2.09 \quad (2)$$

This relationship is the recommended standard for regions with attenuative properties similar to those of Southern California (Bormann and Dewey 2014). Many scales for regions where properties differ have been published in recent years, for example, see Table 6.4 in Havskov and Ottemöller (2010). For regions where no local scale is available the Southern California scale is often employed. While a local scale for Ireland is in development (Grannell et al. 2018), the INSN currently still employs the Southern California scale; hence, it is also used for the capability estimates presented in this work.

In order to compute network capability at each grid point, the background noise amplitudes d at the station locations have to be known, see step 3 above. In seismic observatories, these are usually available in quasi real-time. This allows for the calculation of network capability in quasi real-time, for example, by using the 5-min root mean square (RMS) of station noise amplitudes. Determining noise amplitudes for the calculation of annual or seasonal network capability is less straightforward. In order to exclude high amplitude events, for example, earthquakes or system artefacts, it is advantageous to employ statistical methods. Many observatories routinely determine statistical properties of seismic data, typically by calculating power density functions (PDF) of power spectrum densities (PSD) in the frequency domain, for example, with the software PQLX (McNamara and Boaz 2011) or the PPSD routine in ObsPy (Krischer et al. 2015).

For this study, we employ PQLX to calculate PSDs, see, Möllhoff and Bean (2016a) for details and Fig. 2, for a sample PDF of the vertical component data of station IGLA, located on the west coast of Ireland (see, Fig. 3). The probability of occurrence of a given power at a particular period is plotted in a color code. Also shown are the statistical quantities mode (black solid line), mean (black-dotted line),

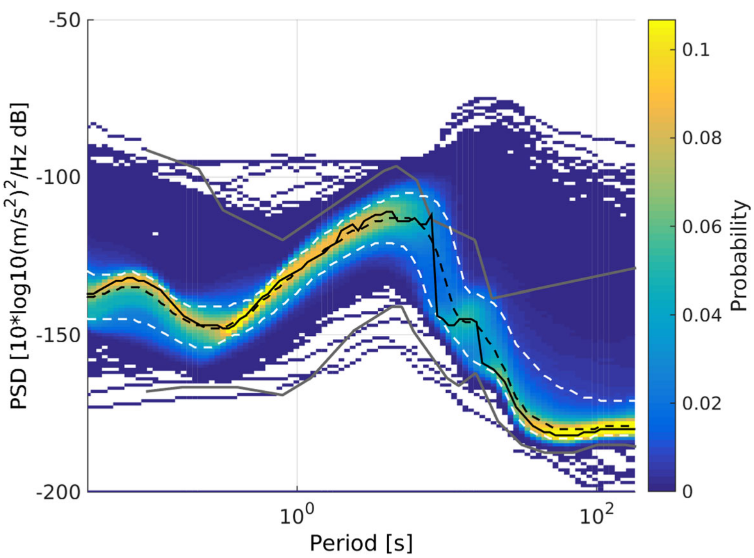

Fig. 2 Representation of power spectrum densities (PSD) as power density functions (PDF) for vertical component data of station IGLA (see, Fig. 3) for the time period January 1, 2010 to March 31, 2017. Also shown are the statistical quantities mode (black solid line), mean (black dotted line), 90 percentile (P90, upper dashed white line), and 10 percentile (P10, lower dashed white line). The Peterson (1993), New High, and Low Noise Models (NHNM and NLNM) are shown as gray solid lines

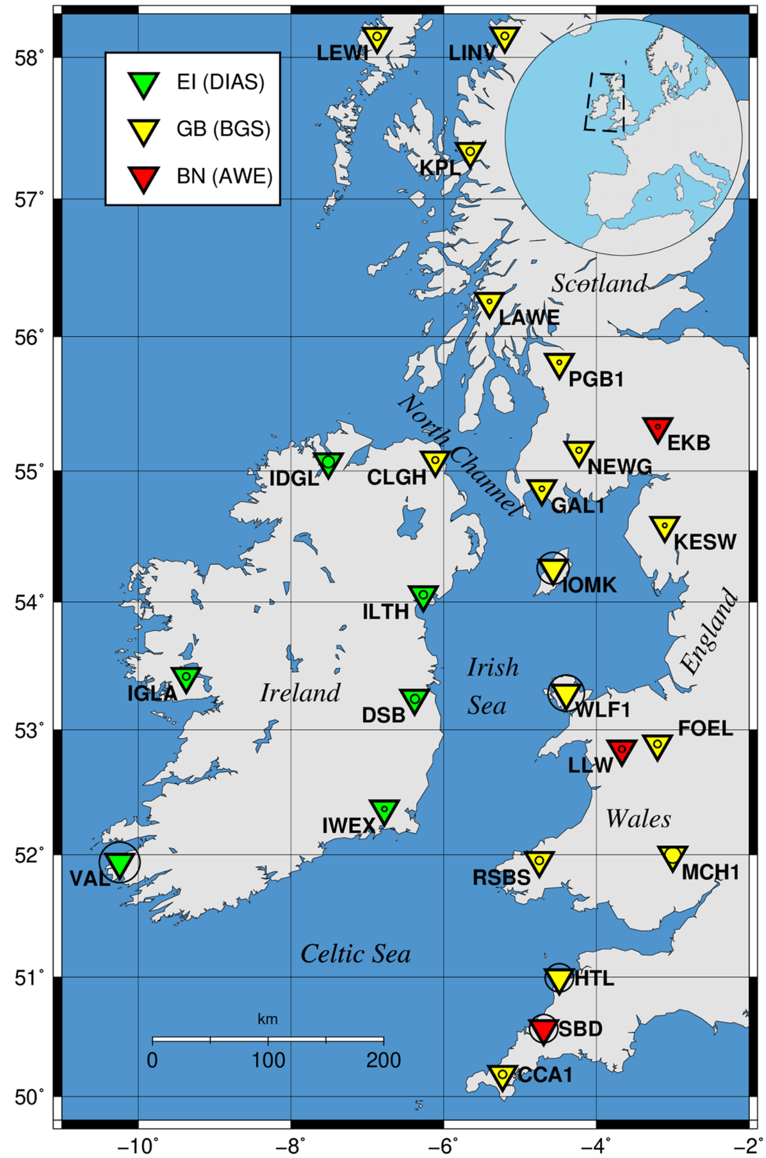

Fig. 3 Map showing seismic stations from which data are used for quasi real-time event detection at the Irish National Seismic Network (INSN (1993)). Stations of the INSN are marked with green triangles, stations of the Great Britain Seismograph Network (GB) are marked with yellow triangles and stations of the Blacknest Array (BN) are marked with red triangles. The long-term station noise levels at 5 Hz center frequency are indicated by circles with a diameter proportional to the P90 value, for example, 0.81 nm at IDGL and 2.82 nm at VAL. Geographical names are in italic type font. The dashed line in the inset shows the location of the depicted region with respect to Europe

90 percentile (P90, upper dashed white line), and 10 percentile (P10, lower dashed white line). The Peterson (1993), New High, and Low Noise Models (NHNM and NLNM) are shown as gray solid lines. The calculated PSD values are based on acceleration power spectra P_a. However, for the calculation of the minimum detectable M_L of a network ground displacements in the time domain are required. These can be obtained by considering a narrow frequency band of interest using the relationship between average peak amplitude displacement d_{ap} and displacement power spectra P_d (Havskov and Alguacil 2006) as follows:

$$d_{ap} = 1.25\sqrt{P_d \cdot (f_2 - f_1)} \tag{3}$$

where f_2 and f_1 are the upper and lower limits of the chosen frequency band of an n-octave filter with geometric center frequency f_0 as follows:

$$f_1 = f_0 2^{-n/2} \qquad f_2 = f_0 2^{n/2} \tag{4}$$

Havskov and Alguacil (2006) have shown that Eq. 3 underestimates displacements by a factor of about

3 when calculating them from PSD values because the latter correspond to maximum amplitudes in the considered time window rather than average peak amplitudes. Taking this into account and using the relationship $P_d = P_a/(2\pi f_0)^4$, it follows:

$$d \approx 3 \cdot d_{ap} = \frac{3.75}{(2\pi f_0)^2} \cdot \sqrt{P_a \cdot (f_2 - f_1)} \qquad (5)$$

This equation allows for a straightforward calculation of noise amplitude displacements d at each station from the corresponding PDF. The resulting values are then used to determine network capability for each grid point, see step 3 above. Using for example, the mode values of the PDF results in the most likely detection capability of a network and using P90 values results in a worst-case scenario network capability. The latter is appropriate when estimating the lowest detectable magnitude of a network for longer time periods because in such cases, it is necessary to also consider times when noise levels were relatively high. An example of such a long-term network capability estimation is given in the following section, where we compare capability maps calculated for the INSN with actual earthquake recordings. Following this, we present examples of applying SN-CAST to assess changes in network geometry, for example, due to station failures and a planned network expansion.

3 Long-term network capability estimation

As an example of calculating the long-term detection capability of a seismic network, we present results for the INSN. Event detection is based on data from permanent seismic stations located on the island of Ireland and along the western parts of Scotland, England, and Wales (see, Fig. 3). The stations are operated by the Dublin Institute for Advanced Studies (DIAS, INSN with network code EI), the Great Britain Seismograph Network operated by the British Geological Survey (BGS, network code GB), and the Blacknest Array operated by the UK Atomic Weapons Establishment (AWE, network code BN). The station geometry shown in Fig. 3 exists since August 1, 2014, when station ILTH was commissioned.

For each station, we estimate representative long-term noise amplitudes from PSD P90 curves based on at least one full calendar year of data since August 1, 2014. For the conversion from P_a to d (see, Eqs. 4 and 5), we chose $f_0 = 5$ Hz and $n = 0.5$, i.e., band limits of a half-octave filter. The choice for f_0 is based on the frequency spectra of two representative earthquakes observed during the study period. The spectra are calculated for vertical component velocity data after applying instrument response correction and a 4–20-Hz bandpass filter. This filter band corresponds to the setting used for automatic seismic event detection in the software Seiscomp3 operated by the INSN. Figure 4a shows spectra for the strongest earthquake

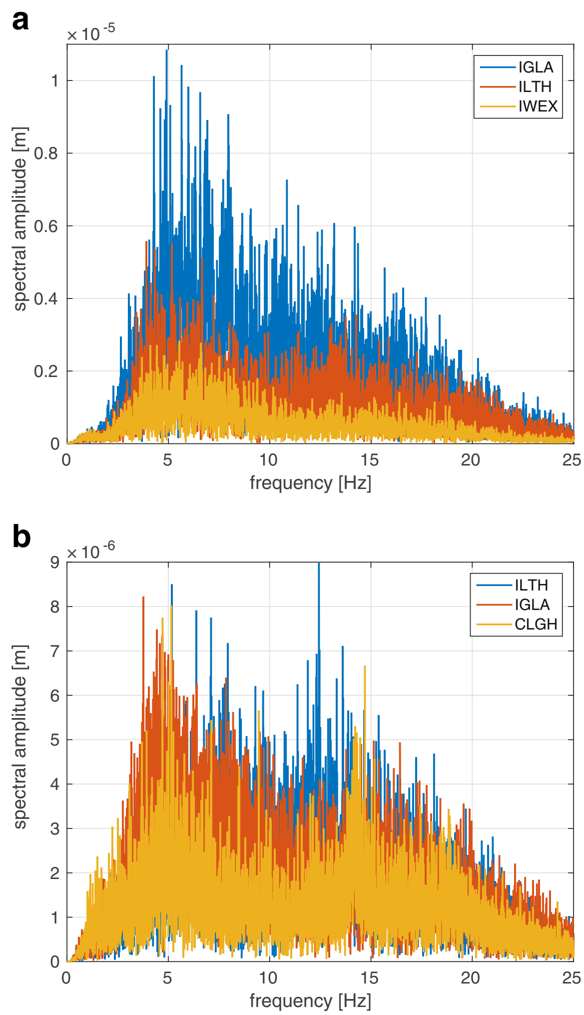

Fig. 4 Spectra of vertical component seismic velocity data after applying instrument response correction and a 4–20-Hz bandpass filter **a** for the magnitude 3.4 earthquake that occurred on January 10, 2016 at 09:47:06 UTC in the Rockall Bank in the Northeast Atlantic and **b** for the magnitude 1.1 earthquake that occurred on September 13, 2016 at 23:07:36 UTC in the northwest of Ireland. See Table 1 for the earthquake parameters and Fig. 5 for the epicenter locations

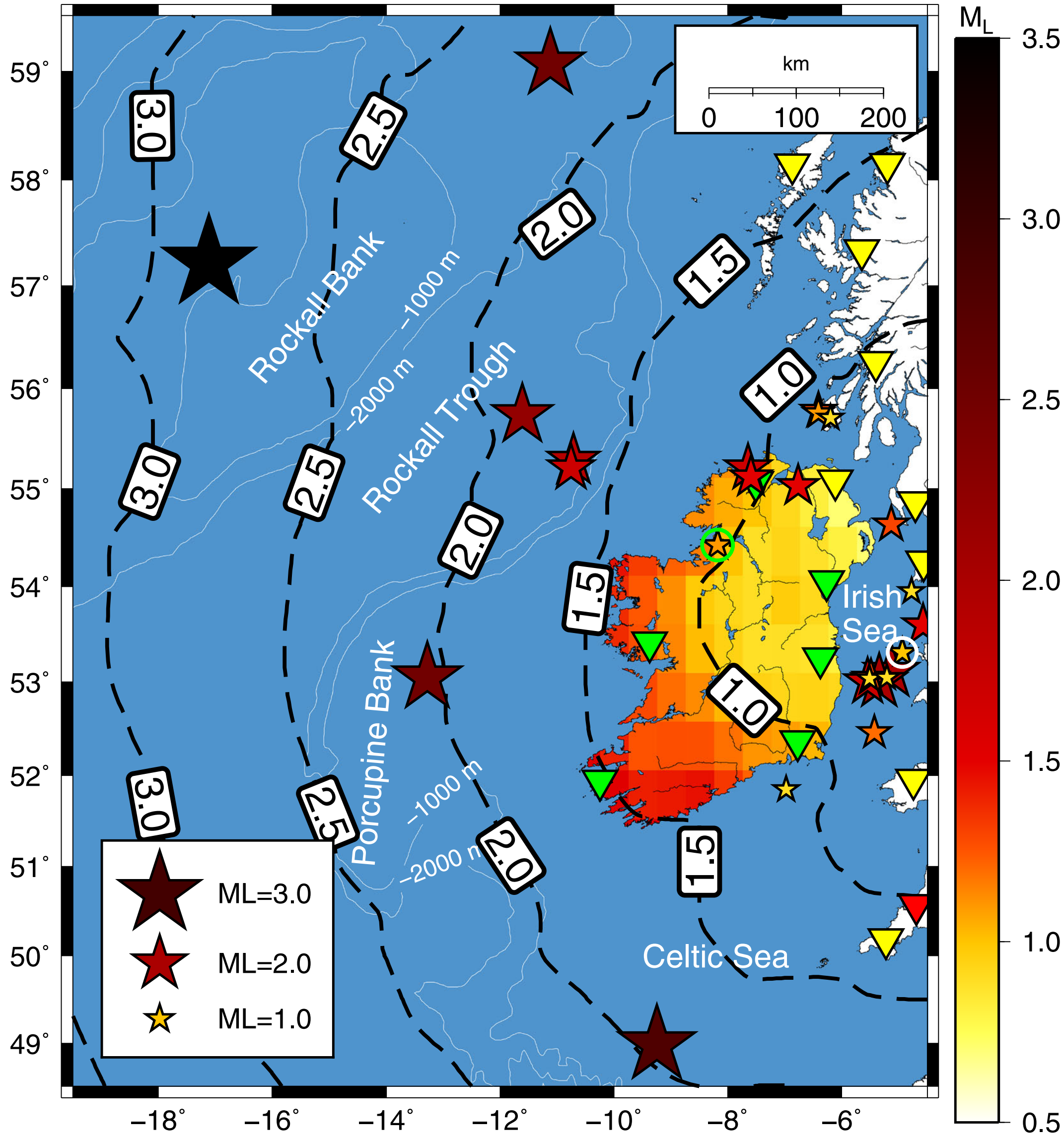

Fig. 5 Geographical distribution of the minimum detectable M_L in Ireland and surrounding seas, based on measured P90 station noise levels and assuming event detections by at least four stations with a SNR > 3. Star symbols present the locations and magnitudes of earthquakes recorded by the INSN between 1.8.2014 and 1.10.2018. Waveforms for the event marked by a green circle are shown in Fig. 6 and those for the event marked by a white circle are shown in Fig. 7. Geographical names are in white font

observed in the study region, namely a magnitude 3.4 event at the Rockall Bank (see, Fig. 5) for the epicenter location and Table 1 for the earthquake parameters. Figure 4b shows spectra for the weakest earthquake observed onshore Ireland; the epicenter location is marked in Fig. 5 with a green circle and the earthquake parameters are given in Table 1. While the spectra for the smaller event show a secondary maximum between 10 and 15 Hz, a main maximum around 5 Hz is observed for both earthquakes. Seismic waveforms for the smaller onshore event are shown in Fig. 6.

We estimate the long-term network capability for the region comprising the island of Ireland and surrounding seas by following the three steps explained in the Method and Implementation section. In step 3, we require that the SNR is larger than 3 on at least four seismic stations. A review of relevant

Table 1 List of parameters for earthquakes reported by the INSN for the time period 1.8.2014 to 1.10.2018

Date (dd.mm.yyyy)	Time (UTC) (hh:mm:ss)	Latitude (degrees)	Longitude (degrees)	M_L	No. of station detections	Location
19.08.2018	14:42:30	55.71	– 6.20	0.9	6	Scotland
25.07.2018	03:26:34	59.07	11.12	2.5	7	North off Rockall Trough
25.06.2018	20:05:50	55.78	– 6.41	1.3	11	Scotland
25.04.2018	19:08:37	53.60	– 4.57	1.5	12	Irish Sea
02.08.2017	05:46:11	55.12	– 7.60	1.5	7	Ireland
18.05.2017	23:04:12	53.05	−5.49	1.3	9	Irish Sea
10.03.2017	05:06:25	53.0	−5.50	1.0	8	Irish Sea
24.01.2017	05:27:47	55.76	– 6.41	1.1	8	Scotland
22.01.2017	08:37:52	55.21	– 10.75	1.7	7	Rockall Trough
08.10.2016	13:11:26	55.03	– 6.77	1.5	9	Ireland
13.09.2016	23:07:36	54.43	– 8.18	1.1	3	Ireland
28.06.2016	00:39:47	52.46	– 5.43	1.2	7	Ireland
10.01.2016	09:47:06	57.22	– 17.11	3.4	8	Rockall Bank
07.01.2016	18:52:24	53.11	– 5.13	2.0	12	Irish Sea
02.11.2015	14:31:37	53.00	– 5.55	1.7	7	Irish Sea
19.09.2015	20:08:27	53.95	– 4.78	0.9	6	Irish Sea
20.08.2015	05:25:22	48.98	– 9.25	2.8	6	Celtic Sea
13.08.2015	04:58:26	51.85	– 6.98	0.9	3	Celtic Sea
31.07.2015	15:38:13	53.00	– 5.34	2.0	8	Irish Sea
09.07.2015	05:12:22	55.74	– 11.61	2.2	9	Rockall Trough
26.06.2015	01:00:39	53.05	– 5.21	0.9	5	Irish Sea
20.05.2015	22:06:08	53.05	– 13.28	2.5	6	Porcupine Bank
11.11.2014	19:56:50	55.29	– 10.71	1.9	5	Rockall Trough
17.10.2014	00:59:59	53.31	– 4.94	1.0	5	Irish Sea
08.09.2014	21:34:08	54.64	– 5.13	1.3	11	North Channel
05.08.2014	05:52:46	55.21	– 7.65	1.7	4	Ireland

literature shows that $N = 4$ is the most common choice with regards to event detection, e.g., Deichmann and Giardini (2009), Horleston et al. (2013), Stork et al. (2014), and Demuth et al. (2016) and many more. More recordings are needed for the reliable location of an event. Trnkoczy et al. (2009), for example, states that “good event records” on at least six stations are a necessary requirement to “provide scientifically credible evidence of an event's location.”

The calculated INSN network capability map is shown together with actual INSN earthquake detections in Fig. 5. Note that the capability is displayed as contours for the entire region and as a colored grid only onshore the island of Ireland. The magnitudes of the detected events are broadly in agreement with the calculated detection limits. In the open North Atlantic, more than 200 km from the north, west, and south coasts of Ireland, only events with $M_L > 2$ are observed. The network capability in this region is not sufficient to detect smaller events that are expected to be present following the Gutenberg-Richter law. Small events with magnitudes $M_L \leq 1$ are only observed in the eastern half of Ireland and nearby seas. The west-east gradient in network capability is not surprising considering that station density around the Irish Sea is highest and much lower on the west coast of Ireland (see, Fig. 3). In the Irish Sea, the calculated detection limit is $M_L \approx 0.8$ (also see the more detailed map in Fig. 8a). This agrees with the fact that the smallest detected event magnitude for the earthquake cluster in the Irish Sea is $M_L = 0.9$ (also see Table 1).

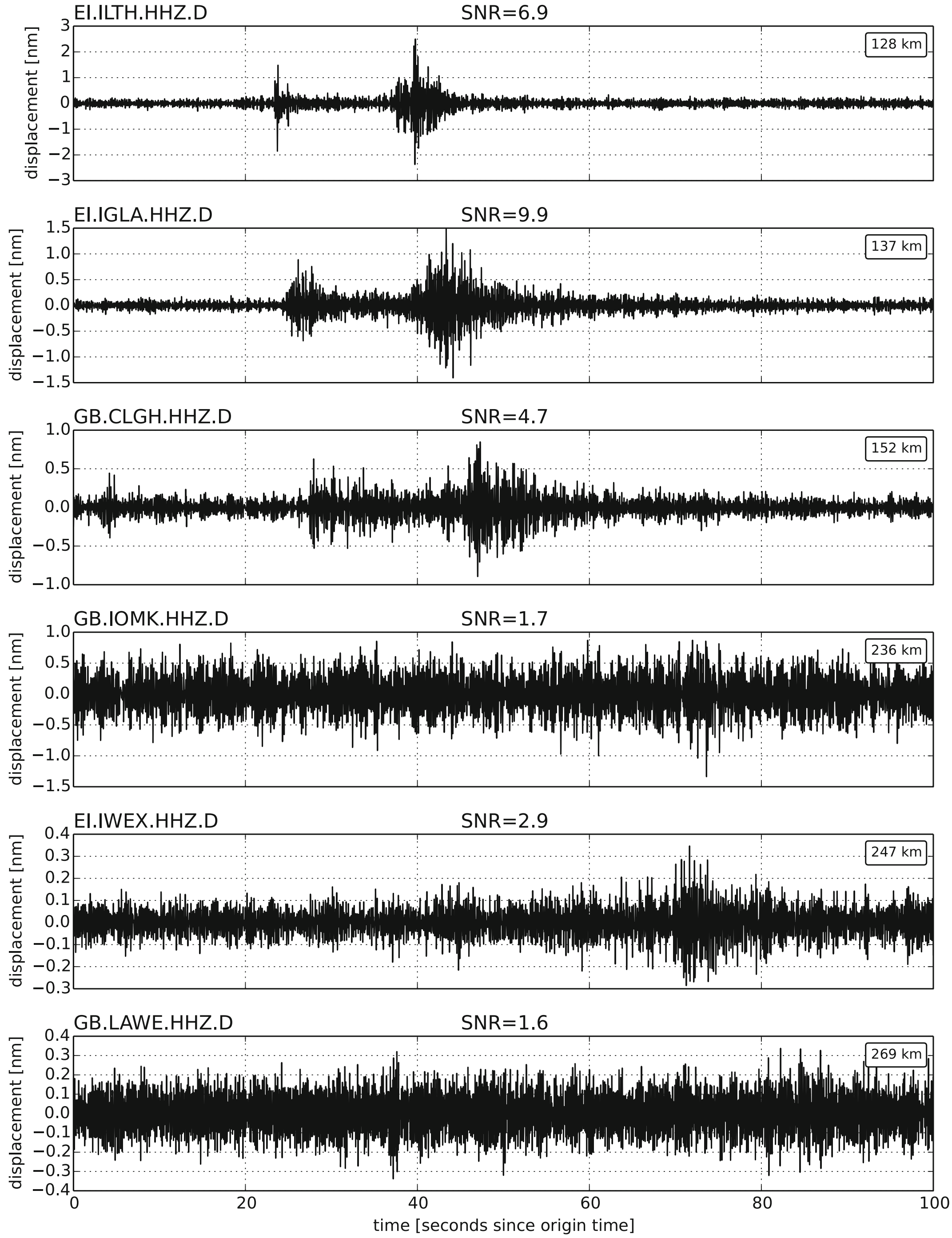

Fig. 6 Seismic waveforms for the $M_L = 1.1$ earthquake that occurred on September 13, 2016 at 23:07:36 UTC onshore, near the northwestern coast of Ireland. The data are filtered with a 4–20-Hz bandpass filter and SNR values are listed above each subfigure. Network, station, and channel names are given for each seismic trace in the top left corner and the hypocentral distance is given in kilometers in the top right corner

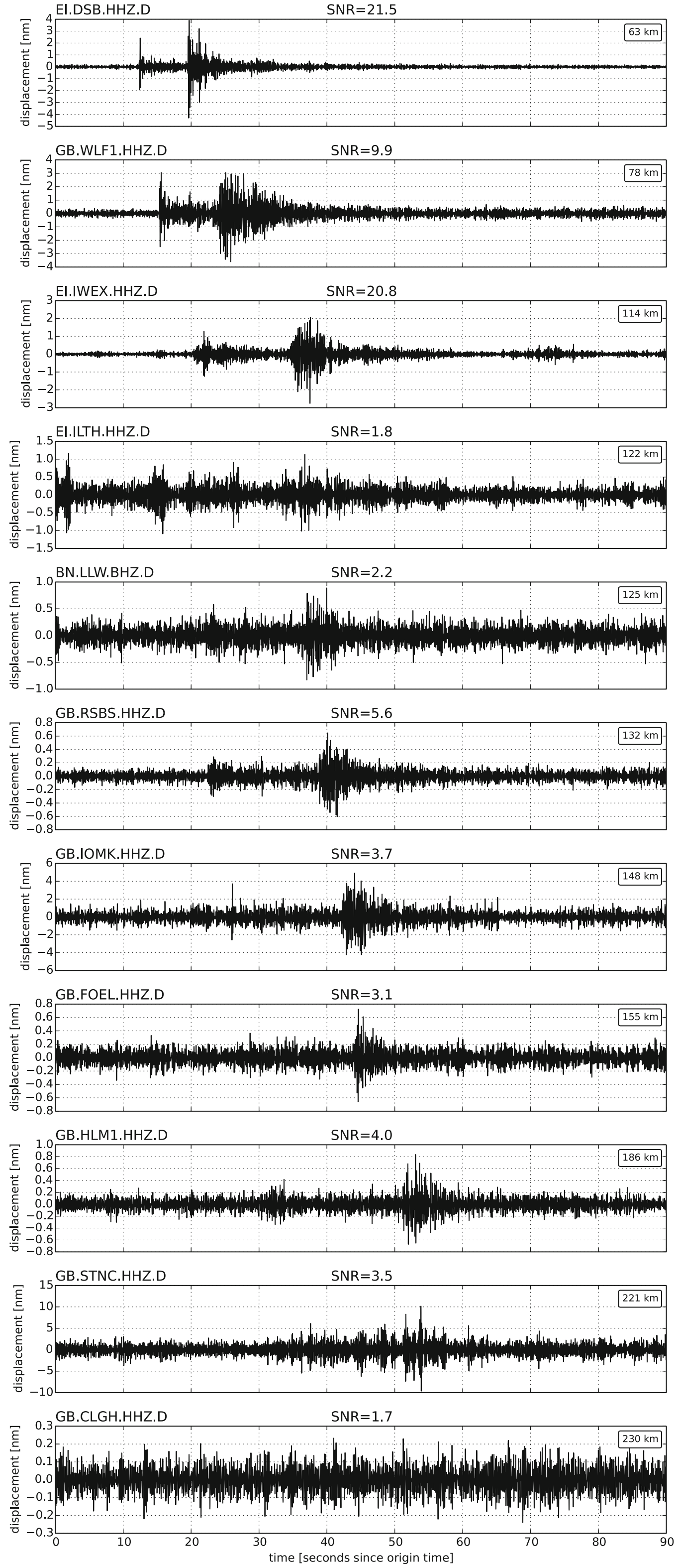

Fig. 7 As Fig. 6 but for the $M_L = 1.0$ earthquake that occurred on March 10, 2017 at 05:06:25 UTC in the Irish Sea. Note the much higher SNR values compared to Fig. 6

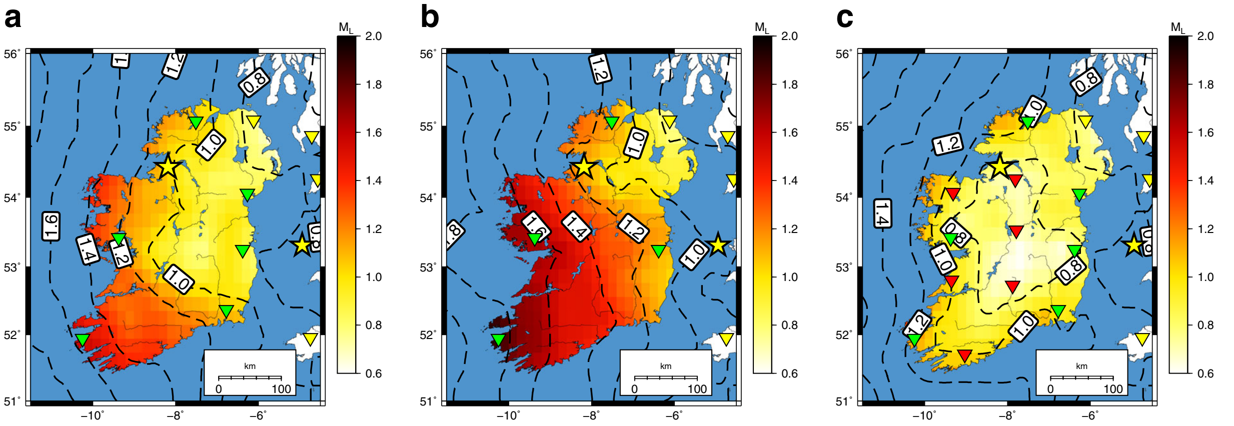

Fig. 8 **a** Detailed map of the minimum detectable M_L in Ireland as shown in Fig. 5. The two stars represent the epicenters for the seismic waveforms shown in Figs. 6 and 7. **b** as (**a**) but assuming two station failures on the east coast of Ireland, namely stations ILTH and IWEX. **c** as (**a**) but assuming the addition of six new stations to the INSN (see, red triangles)

According to the capability map in Fig. 5, the $M_L = 1.1$ event located onshore near the northwest coast of Ireland, marked with a green circle, is expected to be detected with moderate confidence. The seismic recordings for this event (see, Fig. 6), show indeed that the event is detected by 4 stations with SNR values between 2.9 and 6.9. In contrast, the earthquake with $M_L = 1.0$ that occurred on March 10, 2017 in the Irish Sea, marked with a white circle in Fig. 5, is detected by 8 stations with SNR values between 3.1 and 21.5 (see, Fig. 7). This observation is in agreement with the better network capability of $M_L \approx 0.7$ calculated for the corresponding region in the Irish Sea (see, Fig. 8a).

4 Impact of network geometry changes on detection capability

The actual capability of a network varies with time, for example, because of variations in noise levels or because data from some stations might be temporarily unavailable. Here, we present examples that demonstrate how SN-CAST can be used to assess the effect of station failures and the effect of adding new stations to an existing network. Figure 8a shows a detailed map of the calculated INSN detection capability and Fig. 8b shows the reduced capability assuming two station failures on the east coast of Ireland. In most areas, the detection level is reduced by about 0.2 magnitudes. Though this is a relatively small change it does in practice result in a significant reduction of the number of detected quarry blasts, most of which are detected only in the northeastern part of Ireland when all six INSN stations are operational. In Fig. 8c, we show the INSN detection capability that would be expected following an upgrade of the INSN with six additional stations (see, red triangular markers). For most regions, onshore Ireland, the detection limit is expected to improve to values between $M_L = 0.8$ and $M_L = 1.0$. The currently relatively poor network capability of the INSN in the west of Ireland is expected to improve by nearly half a magnitude (compare Fig. 8a with Fig. 8c). Significant network improvements would also be expected for the southern coast of Ireland and the offshore region northwest from Ireland. Several earthquakes have been observed in these two regions in the past (see, the seismicity map at https://www.insn.ie/confirmed (last accessed January 2019)). A better detection capability in these areas would contribute to the better understanding of this seismicity.

5 Conclusion

We present the Seismic Network Capability Assessment Software Tool (SN-CAST) which provides a simple solution to estimate the event detection capability of regional seismic networks. Assuming that the magnitude-distance relationship for the considered region is known the only required input parameters are the seismic station locations and their respective noise levels. Because seismic observatories receive data in quasi real-time SN-CAST can easily be employed to calculate detection capability maps in quasi real-time. Thus, temporal variations in network capability, for example, due to weather events or station malfunctions, can be readily taken into account. Other applications of SN-CAST are to calculate the long-term capability of a network, to estimate the effect of changes in network geometry or to employ it for the design stage of newly proposed networks (see, for example, (Möllhoff and Bean 2016b)). We show examples for the INSN which currently consists of six permanent stations. The average minimum detectable M_L across the island of Ireland is estimated to vary from about $M_L = 0.8$ in the northeast to about $M_L = 1.5$ in the southwest, which is in good agreement with actual observations. We find that the planned doubling of the station number from 6 to 12 will improve the sensitivity of the INSN with a capability between $M_L = 0.8$ and $M_L = 1.0$ in most areas. Along the western coast of Ireland detection limits between $M_L = 1.0$ and $M_L = 1.2$ are expected.

6 Data and resources

The SN-CAST Python code is open source and freely available at http://github.com/moellhoff/sncast (last accessed January 2019). Most of the seismic data used in this study are publicly available and can be downloaded from the European Integrated Data Archive at http://eida.gfz-potsdam.de (last accessed January 2019). Data for some stations in the GB and BN network are private and were obtained from BGS and AWE. The seismic PSD and PDF data were calculated using the software PQLX (McNamara and Boaz 2011). Some plots were generated using the Generic Mapping Tools version 4.5.11 (Wessel et al. 2013), and the seismic waveform plots were generated with the ObsPy software package (Krischer et al. 2015).

Acknowledgements We thank the INSN analysts for their contribution to the generation of the INSN seismic event catalog. We acknowledge the provision of real-time data access to seismic stations from the British Geological Survey (BGS) and the Atomic Weapons Establishment (AWE) Blacknest in the UK. The operation of the INSN was supported by iCRAG in the years 2015–2016 and is supported since November 2017 by the Geological Survey Ireland. The authors are grateful for the constructive review from an anonymous reviewer.

References

Baillard C, Crawford WC, Ballu V, Hibert C, Mangeney A (2014) An automatic kurtosis-based P- and S-phase picker designed for local seismic networks. Bull Seismol Soc Am 104:394–409. https://doi.org/10.1785/0120120347

Bormann P, Dewey JW (2014) The new IASPEI standards for determining magnitudes from digital data and their relation to classical magnitudes. New Manual of Seismological Observatory Practice 2 (NMSOP-2). In: Bormann P (ed) Information sheet 3.3, IASPEI, GFZ german research centre for geosciences. Potsdam, Germany, pp 1–44. https://doi.org/10.2312/GFZ.NMSOP-2_IS_3.3

D'Alessandro A, Badal J, D'Anna G (2013) Location performance and detection threshold of the spanish national seismic network. Pure Appl Geophys 170:1859. https://doi.org/10.1007/s00024-012-0625-y

Deichmann N, Giardini D (2009) Earthquakes induced by the stimulation of an enhanced geothermal system below basel (Switzerland). Seism Res Lett 80:784–798. https://doi.org/10.1785/gssrl.80.5.784

Demuth A, Ottemöller L, Keers H (2016) Ambient noise levels and detection threshold in Norway. J Seismol 20:889. https://doi.org/10.1007/s10950-016-9566-8

Fischer T, Bachura M (2014) Detection capability of seismic network based on noise analysis and magnitude of completeness. J Seismol 18:137. https://doi.org/10.1007/s10950-013-9407-y

Gaci S (2014) The use of wavelet-based denoising techniques to enhance the first-arrival picking on seismic traces. IEEE Trans Geosci Remote Sens 52(8):4558–4563. https://doi.org/10.1109/TGRS.2013.2282422

Grannell J, Arroucau A, Lebedev S, Möllhoff M, Bean CJ (2018) A local magnitude scale for Ireland and its offshore regions. 36th general assembly of the European Seismological Commission, Malta, ESC-S22-957

Havskov J, Alguacil G (2006) Instrumentation in earthquake seismology, Springer, Modern Approaches in Geophysics (Book 22) ISBN: 1402029683

Havskov J, Ottemöller L (2010) Routine data processing in earthquake seismology. Springer, London, New York

Horleston A, Stork A, Verdon J, Baird A, Wookey J, Kendall M (2013) Seismic Monitoring of Drilling Operations in Balcombe, West Sussex. University of Bristol Report

Hutton LK, Boore DM (1987) The ML scale in southern California. Bull Seismol Soc Am 77(6):2074–2094

INSN (1993) Irish national seismic network operated by the Dublin Institute for Advanced Studies. International Federation of Digital Seismograph Networks, Other/Seismic Network. https://doi.org/10.7914/SN/EI

Krischer L, Megies T, Barsch R, Beyreuther M, Lecocq T, Caudron C, Wassermann J (2015) ObsPy: A bridge for seismology into the scientific Python ecosystem. Comp Sci Disc 8(1):014003. https://doi.org/10.1088/1749-4699/8/1/014003

Mahani AB, Kao H, Walker D, Johnson J, Salas C (2016) Performance evaluation of the regional seismograph network in Northeast British Columbia, Canada, for monitoring of induced seismicity. Seism Res Lett 87(3):648–660. https://doi.org/10.1785/0220150241

McNamara DE, Boaz RI (2011) PQLX: A seismic data quality control system description, applications and user manuals. US Geol Surv Open-File Rept 2010-1292:52

Möllhoff M, Bean CJ (2016a) Seismic noise characterization in proximity to strong microseism sources in the Northeast Atlantic. Bull Seismol Soc Am 106(2):464–477. https://doi.org/10.1785/0120150204

Möllhoff M, Bean CJ (2016b) Technical Specification for Sub-regional Seismic Baseline Monitoring. Task 5 in: Environmental Impacts of Unconventional Gas Exploration and Extraction (UGEE), Final Report 2: Baseline Characterisation of Seismicity, Environmental Protection Agency, Co. Wexford, Ireland, ISBN 978-1-84095-688-7, 88–118. https://doi.org/10.13140/RG.2.2.21987.76321

Nanjo KZ, Schorlemmer D, Woessner J, Wiemer S, Giardini D (2010) Earthquake detection capability of the Swiss Seismic Network. Geophys J Int 181:1713–1724. https://doi.org/10.1111/j.1365-246X.2010.04593.x

Peterson J (1993) Observation and modeling of seismic background noise. US Geol Surv Open-File Rept 93–322

Richter CF (1935) An instrumental earthquake magnitude scale. Bull Seismol Soc Am 25:1–32

Schultz R, Stern V, Gu YJ, Eaton D (2015) Detection threshold and location resolution of the Alberta Geological Survey earthquake catalogue. Seism Res Lett 86(2A):385–397. https://doi.org/10.1785/0220140203

Stabile TA, Iannaccone G, Zollo A, Lomax A, Ferulano MF, Vetri MLV, Barzaghi LP (2013) A comprehensive approach for evaluating network performance in surface and borehole seismic monitoring. Geophys J Int 192(2):793–806. https://doi.org/10.1093/gji/ggs049

Stork AL, Verdon JP, Kendall JM (2014) The robustness of seismic moment and magnitudes estimated using spectral analysis. Geophys Prospect 62:1365–2478. https://doi.org/10.1111/1365-2478.12134

Trnkoczy A, Havskov J, Ottemöller L (2009) Seismic Networks. in new manual of seismological observatory practice (NMSOP-2). In: Bormann P (ed) IASPEI, GFZ German research centre for geosciences. Potsdam, Germany, pp 1–34. https://doi.org/10.2312/GFZ.NMSOP_r1_ch8

Wessel P, Smith WHF, Scharroo R, Luis JF, Wobbe F (2013) Generic mapping tools: improved version released. EOS Trans AGU 94:409–410